forests

MDPI

Article

Chloroplast Spacer DNA Analysis Revealed Insights into Phylogeographical Structure of *Phoebe chekiangensis*

Xiankun Wu [1,2,3], Yan Chen [4], Chenhui Nan [2,3], Shucheng Gao [1], Xiangzhen Chen [1] and Xiangui Yi [1,*]

[1] Co-Innovation Center for Sustainable Forestry in Southern China, College of Life Sciences, Nanjing Forestry University, Nanjing 210037, China; 107103@nfpc.edu.cn (X.W.); 18762143959@163.com (S.G.); chenxiangzhen0508@163.com (X.C.)
[2] Faculty of Criminal Science & Technology, Nanjing Forest Police College, Nanjing 210023, China; nanchenghui@126.com
[3] Key Laboratory of State Forest and Grassland Administration Wildlife Evidence Technology, Nanjing 210023, China
[4] Zhongshan Cemetery Management Bureau, Nanjing 210037, China; txtangxia@163.com
* Correspondence: yixiangui@njfu.edu.cn

Abstract: Research studies on the conservation genetics of endangered plants play a crucial role in establishing management plans for biodiversity conservation. *Phoebe chekiangensis* is a precious and scarce tree species resource in the East China region. To comprehend the origin, evolutionary history, geographical, and historical factors that has contributed to the current distribution pattern of *Phoebe chekiangensis* in the East China region, we conducted a phylogeographic analysis that utilized intergenic spacers of chloroplast DNA (cpDNA). We amplified and sequenced three spacer regions of cpDNA (*psbC-trnS*, *trnL-Intro*, and *Ycf3*) intergenic spacer regions of 306 individuals from 11 populations, encompassing the majority of its geographical range in China. Our analysis revealed a total of 11 haplotypes. The research findings show that the spacer regions of the cpDNA genetic diversity of *Phoebe chekiangensis* was H_d = 0.423, and the nucleotide diversity was $P_i \times 10^{-3}$ = 0.400. At the species level, the population differentiation index F_{st} = 0.25610 ($p < 0.05$), and the gene flow N_m = 0.73. The genetic variation between populations was 29.14%, while within populations, it was 70.86%, with the inter-population genetic variation much lower than the within-population variation. The divergence time between the genera *Phoebe* and *Machilus* was estimated to be approximately 37.87 mya (PP = 1; 95%HPD: 25.63–44.54 mya), and the crown group time of the genus *Phoebe* was estimated to be 21.30 mya (PP = 1; 95%HPD: 9.76–34.94 mya). The common ancestor of the 11 *Phoebe chekiangensis* haplotypes was 7.85 mya, while the H7, H8, and H10 haplotypes of *Phoebe chekiangensis* (northern region) differentiated relatively late, with a divergence time of 1.90 mya. Neutrality tests (NTs) and mismatch distribution analysis (MDA) suggest that the time frame for *Phoebe chekiangensis* to expand southwestward along Wuyishan was relatively short and its adaptability to the environment was low, thereby limiting the formation of new haplotypes. These results suggest that *Phoebe chekiangensis* exhibited greater adaptation to the northern subtropics than to the central subtropics, offering valuable insights for the conservation and utilization of germplasm resources.

Keywords: Lauraceae; spacer regions of cpDNA; population genetic structure and diversity; phylogeography

Citation: Wu, X.; Chen, Y.; Nan, C.; Gao, S.; Chen, X.; Yi, X. Chloroplast Spacer DNA Analysis Revealed Insights into Phylogeographical Structure of *Phoebe chekiangensis*. *Forests* **2024**, *15*, 1073. https://doi.org/10.3390/f15071073

Received: 29 April 2024
Revised: 13 June 2024
Accepted: 14 June 2024
Published: 21 June 2024

1. Introduction

Phoebe chekiangensis C. B. Shang is an exclusive species found in China and belongs to the family Lauraceae and the genus *Phoebe* Nees [1,2]. It has dispersed populations in the evergreen broad-leaved forests of the eastern subtropics. The species has a limited distribution range, low population and individual counts, and faces significant habitat fragmentation [3]. It stands as a precious and scarce tree species resource in the East China region [4]. Revealing the refuge locations and migration routes is crucial in studying

plant responses to Pleistocene climate changes and understanding the current species' geographical distribution patterns [5,6].

Sequencing cpDNA spacers aids in analyzing plant evolutionary relationships and predicting the geographic ranges of species based on [7,8]. The spacer regions of cpDNA harbor genetic information, representing a monophyletic and non-recombinant genetic unit that is valuable for conducting phylogeographic analyses of species [9]. Mutation rates vary in different regions of the genome, with most variations occurring in large single-copy regions rather than in inverted repeat sequences [9–11]. Moreover, due to its relatively high genetic variation, chloroplast DNA is frequently utilized for inferring the genetic relationships between species, estimating their divergence times, and occasionally characterizing germplasm [12]. Its genetic lineage tends to form a monophyletic group, making it possible to use spacer regions of cpDNA analysis methods to discuss the phylogeographic structure and population historical dynamics of *Phoebe chekiangensis*, thus estimating the divergence time and population expansion time of *Phoebe chekiangensis* genetic lineages [13,14].

In this study, by reading the relevant papers on the genus *Phoebe*, the haplotype variation, distribution, and polymorphism of the sampled populations were analyzed based on the examination of three spacer regions of cpDNA spacer sequences (*psbC-trnS*, *trnL-Intro*, *ycf3*) [15–18]. A haplotype tree was constructed to investigate the genetic structure and diversity of *Phoebe chekiangensis* populations [19]. Geographical grouping of the *Phoebe chekiangensis* populations was conducted by estimating the phylogeny and evolutionary time of cpDNA haplotypes [20]. Historical and dynamic analysis was utilized to determine potential spatial and population expansions in various geographical clusters, along with the timing of such events [21].

2. Materials and Methods

2.1. Plant Materials and DNA Extraction

A total of 306 individual trees of *Phoebe chekiangensis* were collected from 11 populations (10 wild populations and 1 cultivated population sample) that covered basically all the distribution areas in China (Table 1). Fresh young leaves were collected from 14 to 38 sample trees, with a minimum distance of 100 m apart from each other. The leaf samples were then dried using silica gel for DNA extraction using a commercial kit DP305 (Tiangen Biotechnology Co., Ltd., Shanghai, China) by following the manufacturer's instructions [22].

Table 1. The geographical origin and sampling information of *Phoebe chekiangensis* populations.

NO.	Pop. Label	Location	Longitude/E	Latitude/N	Altitude/m	Pop. Size
1	JBX	Junbu Township, Yongfeng, Jiangxi Province	115.696	26.727	230	30
2	YQLC	Yanquan Forest farm, Fuzhou, Jiangxi Province	116.927	27.043	308	22
3	WYSZ	Wuyishan town, Shangrao, Jiangxi Province	117.875	28.018	434	30
4	LXC	Luxi village, Huangshan, Anhui Province	117.489	29.698	86	30
5	LZLC	Laizhou experimental forest farm, Fujian Province	118.002	26.638	210	22
6	TM	Tianmu Mountain, Hangzhou, Zhejiang Province	119.443	30.322	342	38
7	DGC	Qingyuan, Zhejiang Province, Zuoxi Daigen village	119.345	27.593	652	30
8	LS	Songyang Pankeng village, Qingyuan, Zhejiang Province	119.400	28.395	329	30
9	SXJ	Zhejiang Taizhou Shenxian Residence (cultivation)	120.590	28.680	208	30
10	LAS	Li'an Mountain, Hangzhou, Zhejiang Province	120.109	30.209	56	30
11	NB	Tiantong Mountain, Ningbo, Zhejiang Province	121.792	29.801	115	14
Total						306

2.2. Chloroplast DNA, Amplification, Sequencing, and Sequence Alignment

Three cpDNA spacer regions were utilized for analyzing sequence variation within and between populations of Phoebe chekiangensis: *psbC-trnS*, *trnL-Intro*, and *Ycf3* [18,23,24].

A 25 µL PCR amplification reaction included a DNA template, 0.5 µL of each upstream and downstream primers (10 µmol/L each, as specified in Table 2), 12.5 µL of 2 × PCR Master Mix, and 9.5 µL of ddH2O. The PCR amplification procedure comprised an initial denaturation at 94 °C for 5 min, followed by 30 cycles of denaturation at 94 °C for 1 min, annealing at 54–56 °C for 1 min, extension at 72 °C for 1 min, and a final extension at 72 °C for 5 min. Post-PCR, the samples underwent purification and sequencing at China Shanghai BioEngineering upon satisfying the standards after 1% agarose gel electrophoresis. The spacer regions' cpDNA sequences were aligned using MAFFT version 7 [25], manually reviewed, and edited with PhyloSuite version 1.2.2. Subsequently, the *psbC-trnS*, *trnL-Intro*, and *Ycf3* sequences were concatenated (Table 2).

Table 2. The information about primers.

Primer		Primer Sequence	References
psbC-trnS	F:	GCAGCTGCAGCAGGATTTG	Qiao et al., 2019 [23]
	R:	GGAGAGATGGCCGAGTGGTT	
trnL-Intro	F:	CGAAATCGGTAGACGCTACG	Qiao et al., 2019 [23]
	R:	GGGGATAGAGGGACTTGAAC	
Ycf3	F:	AGAACCGTACTTGAGAGTTTCC	Makhmudjanov et al., 2023 [18,23]
	R:	CTGTCATTACGTGCGRCTATCT	

2.3. Genetic Diversity, Haplotype Network Construction, and Haplotype Distribution

The population genetic diversity, which was assessed through 3 cpDNA fragments, was characterized using nucleotide diversity (π), haplotype diversity (H_d), genetic differentiation coefficient (F_{st}), gene flow, and the number of haplotypes by utilizing DnaSP version 5.0 software. A chloroplast haplotype relationship analysis was conducted using a default median-joining network in NETWORK 5.0 [26]. The distribution of all haplotypes was mapped onto a relief map of China, with specific clades identified on the chloroplast network.

2.4. Population Genetic Structure

The genetic differentiation within and between populations of *Phoebe chekiangensis* was investigated using the AMOVA analysis in Arlequin software version 3.5 [27]. Furthermore, Pennut was utilized to compute N_{st} and G_{st} values from the cpDNA spacer region data, identifying potential significant geographical lineage structures within the *Phoebe chekiangensis* population. Arlequin was applied for neutral testing and mismatch analysis to examine whether the *Phoebe chekiangensis* population had undergone bottleneck or expansion events. In molecular variance analysis (AMOVA), F_{st} (the proportion of genetic variation between populations and groups overall) is commonly used to assess the genetic differentiation between populations, with values ranging from [0, 1]. When $F_{st} = 1$, alleles tend to be stable within populations, indicating complete differentiation; when $F_{st} = 0$, it indicates no differentiation between populations; when F_{st} is less than 0.15, there is low genetic differentiation between populations; when $0.15 \leq F_{st} < 0.25$, it is considered moderate; and when F_{st} is greater than or equal to 0.25, it is high. Thus, the higher the F_{st} value, the greater the genetic differentiation between populations.

2.5. Phylogenetic Analyses and Divergence Time Estimation

The phylogenetic tree was reconstructed using PAUP Version 4.0 [28] through maximum likelihood (ML) analysis, as well as MrBayes Version 3.1.2 [29] through Bayesian analysis. *Machilus oreophila* and *Machilus nanmu* styraciflua sequences were designated as the outgroup. The Markov chain Monte Carlo (MCMC) ran for 10,000,000 generations, sampling every 1000 generations. A total of 10,000 trees were excerpted, with the initial 2500 trees being discarded as the burn-in. The remaining trees were used to construct a 50% consensus tree and calculate the posterior probabilities. Using the Bayesian method (BI) and the maximum likelihood (ML) method to construct 11 haplotype phylogenetic trees,

the Bayesian method constructed the optimal nucleotide substitution model HKY+F+I; the maximum likelihood method's optimal nucleotide substitution model was TPM3u+F+I. The finalized tree was edited and visualized with FIGTREE v1.4.0 [30].

The divergence time of all haplotypes was estimated by BEAST Version 1.7.4 [31], with the uncorrelated lognormal (UCLN) relaxed clock model. Five independent runs of 80,000,000 MCMC generations were conducted, sampling at every 8000 generations, following a burn in of the first 10% cycles. The log files were checked in TRACER v.1.6 [32] to confirm that the effective sample size (ESS) for all parameters reached adequacy (ESS > 200) and convergence of the chains to a stationary distribution. Divergence time and 95% highest posterior density (HPD) were visualized using FIGTREE v1.4.0 [30].

We constructed a phylogenetic tree at the family level of Lauraceae after downloading the NCBI website sequences of 3 *Alseodaphne* species: *Alseodaphne semecarpifolia* (MG407595), *A. gracilis* (MG407593), and *A. huanglianshanensis* (MG407594); 1 *Persea americana* (ON641344) from the *Persea* genus; 4 *Machilus* species: *M. pauhoi* (MH178403), *M. thunbergii* (MH178404), *M. yunnanensis* (KT348516), and *M. balansae* (KT348517); 5 *Cinnamomum* species: *Cinnamomum camphora* (LC228240), *C. verum* (NC_035236), *C. parthenoxylon* (MH050971), *C. micranthum* (KT833081), and *C. yabunikkei* (NC_044864); and 6 species of the *Phoebe* genus. A total of 19 Lauraceae cp DNA sequences were used to construct a phylogenetic tree at the level of some genera within the family using three molecular clocks.

2.6. Tests of Expansion

Neutrality tests (Tajima's and Fu's FS tests) and pairwise mismatch distribution analyses were carried out using Arlequin, version 3.1 [27]. The expected and observed value curves from DnaSP version 5.0 were compared to assess the hypothesis of sudden population expansion when they aligned. Significant negative values of Tajima's D and Fu's Fs may indicate population expansion. Fu's Fs, being more sensitive than Tajima's D, is commonly preferred as the test parameter. The neutrality test (NT) follows the neutral theory, assuming molecular mutations are either neutral or nearly neutral, having no species advantage or disadvantage. It dismisses natural selection effects, attributing mutation outcomes to random genetic drift within the population, making the nucleotide substitution rate equivalent to the mutation rate. Negative and statistically significant results of Tajima's D and Fu's Fs ($p < 0.05$) suggest recent population expansion or bottleneck events. Mismatch distribution analysis (MDA) predominantly determines past population expansion events by examining the base distribution disparities between haplotypes.

3. Results

3.1. Sequence Variation and Haplotype Frequency

The total length of the three chloroplast DNA fragment sequences was 1548 bp, with the *psbC-trnS* fragment being 491 bp, the *trnL-Intro* fragment being 483 bp, and the *ycf3* fragment being 574 bp. A total of nine polymorphic sites, with two each in the *psbC-trnS* and *trnL-Intro* fragments, and five in the *ycf3* fragment. In terms of the geographic haplotype statistics, a total of 11 haplotypes were detected among the 11 populations (Table 3).

Based on the above polymorphic sites, the following numbers of haplotypes were found: The population of Tiantongshan (NB) in Ningbo, Zhejiang, had six haplotypes. The populations in Laizhou Experimental Forest Farm (LZLC) in Fujian and Li'anshan (LAS) in Hangzhou, Zhejiang, each had three haplotypes. The populations in Junbu Township (JBX) in Yongfeng, Jiangxi; Yanquan Forest Farm (YQLC) in Fuzhou, Jiangxi; Luxi Village (LXC) in Qimen, Anhui; and Shenxianju (SXJ) in Taizhou had two haplotypes. The remaining populations had only 1 haplotype (Table 4). The single haplotypes H3 and H8 only appeared once in different populations; haplotype H1 appeared in all populations with the highest frequency (230/306), followed by H5 (19/306), with 81.4% of individuals possessing these two haplotypes. At the species level, *Phoebe chekiangensis* exhibited a low level of haplotype diversity (H_d = 0.423) and nucleotide diversity (P_i = 0.400). Across the entire distribution range, the range of haplotype diversity varied from 0.000 to 0.846,

with the nucleotide diversity ranging from 0.000 to 1.910 in different populations of *Phoebe chekiangensis*. Populations in Tiantongshan (NB) in Ningbo, Laizhou Experimental Forest Farm (LZLC) in Fujian, and Li'anshan (LAS) in Hangzhou, Zhejiang, each contained three or more haplotypes, showing higher values for the haplotype diversity parameter Hd. The highest haplotype genetic diversity parameter was H_d = 0.846 in Ningbo's Tiantongshan (NB), while the lowest was H_d = 0.000 in Tianmushan (TM) in Lin'an, Zhejiang.

Table 3. Haplotype sequence variation of 3 spacer regions of cpDNA fragments detected in *Phoebe chekiangensis*.

Haplotype	00101	00516	00517	00525	00705	00870	00889	00903	00933	10189	11048	11447	11545	11641	Distribution Quantity (No.)
	trnL-Intro					Ycf3					psbC-trnS				
Hap1	C	A	A	G	A	C	C	C	C	G	G	G	A	G	230
Hap2	·	·	·	·	·	·	·	·	·	·	A	·	·	·	26
Hap3	G	·	·	·	·	·	·	·	·	·	·	·	·	·	12
Hap4	·	·	·	·	·	·	·	·	·	A	·	·	·	·	6
Hap5	·	·	·		C	·	·	·	·	·	·	·	·	·	19
Hap6	·	·	·	·	·	T	·	·	·	·	·	·	·	·	4
Hap7	·	·	·	·	·	·	·	·	T	·	·	·	·	·	2
Hap8	·	G	G	T	·	·	·	·	T	·	·	·	·	·	2
Hap9	·	·	·	·	·	A	A	A	·	·	·	·	·	·	2
Hap10	·	·	·	·	·	T	·	·	T	·	·	·	·	·	2
Hap11	·	·	·	·	·	·	·	·	·	·	·	A	G	A	1

Table 4. Geographic distribution information and genetic diversity parameters of *Phoebe chekiangensis* by spacer regions of cpDNA analysis.

	Population Code	Pop. Size	H_d	Pi × 10^{-3}	K	Haplotypes/Ribotypes (No. of Individuals)
1	JBX	30	0.524	0.360	0.497	H1 (18), H2 (12)
2	YQLC	22			0.524	H1 (11), H2 (11)
3	WYSZ	30	0.186	0.130	0.186	H1 (30)
4	LS	30	0.331	0.230	0.331	H1 (30)
5	DGC	30	0.186	0.130	0.186	H1 (30)
6	SXJ	30	0.186	0.130	0.186	H1 (27), H2 (3)
7	LZLC	22	0.714	0.660	0.961	H1 (9), H4 (6), H5 (7)
8	LXC	30	0.497	0.340	0.497	H1 (18), H3 (12)
9	TM	38	0.000	0.000	0.000	H1 (38)
10	LAS	30	0.625	0.510	0.736	H1 (14), H5 (12), H6 (4)
11	NB	14	0.846	1.910	2.758	H1 (5), H7 (2), H8 (2), H9 (2), H10 (2), H11 (1)
Northern region (LXC, TM, LAS, NB)		112	0.551	0.640	0.652	H1 (75), H3 (12), H5 (12), H6 (4), H7 (2), H8 (2), H9 (2), H10 (2), H11 (1)
Southern region (JBX, YQLC, WYSZ, LZLC, DGC, LS, SXJ)		194	0.295	0.330	0.473	H1 (155), H2 (26), H4 (6), H5 (7)
All		306	0.423	0.400	0.562	

Based on the distribution patterns, the 11 haplotypes could be classified into two regions. The northern region, roughly located in the northern subtropics of the Hanggan tectonic zone, included four populations: Luxi Village (LXC) in Qimen, Anhui; Tianmushan (TM) in Zhejiang; Li'anshan (LAS) in Hangzhou; and Tiantongshan (NB) in Ningbo; while

the remaining seven populations were in the southern subtropics on the south side. Regional level analysis showed that the range of haplotype diversity in the northern and southern regions was from 0.295 to 0.551, while the range of nucleotide diversity was from 0.330 to 0.640, with genetic diversity in the populations of the northern region being higher than those in the southern region.

3.2. Haplotype Distribution and Geographical Distribution Pattern

The results show that among the 11 haplotypes of *Phoebe chekiangensis*, only H1, H2, and H5 were shared haplotypes. Among them, H1 was present in all 11 populations, with the highest proportion in each population, including a total of 128 individuals (41.8%), such as in Jiangxi Wuyishan Town (WYSZ), Zhejiang Daigen Village (DGC), Zhejiang Lishui Pankeng Village (LS), and Zhejiang Tianmu Mountain (TM), where H1 was the only haplotype. Further analysis could be conducted in conjunction with the habitat and potential migration routes to explore causes (Figure 1). H2 was a shared haplotype among three populations, containing 26 individuals, while H5 was shared among two populations, with 19 individuals. In all populations, the number of individuals with unique haplotypes was less than six, demonstrating rare unique haplotypes. Unique haplotypes included H4, H6, H7, H8, H9, H10, and H11, with H4 unique to the Fujian Laizhou Experimental Forest (LZLC) population; H6 unique to the Zhejiang Hangzhou Lianshan (LAS) population; and H7, H8, H9, H10, and H11 unique to the Ningbo Tiantongshan (NB) population, with a total of only nine individuals among these five haplotypes. This indicates that except for the Ningbo Tiantongshan (NB) population, the habitats of the populations where these haplotypes were found were quite similar or had not formed good geographical isolation, resulting in relatively homogeneous haplotype compositions. As the population located at the easternmost distribution of *Phoebe chekiangensis*, the habitat of the Ningbo Tiantongshan (NB) population was near the East China Sea, differing from the habitats of other populations, which may have led to the formation of more new haplotypes.

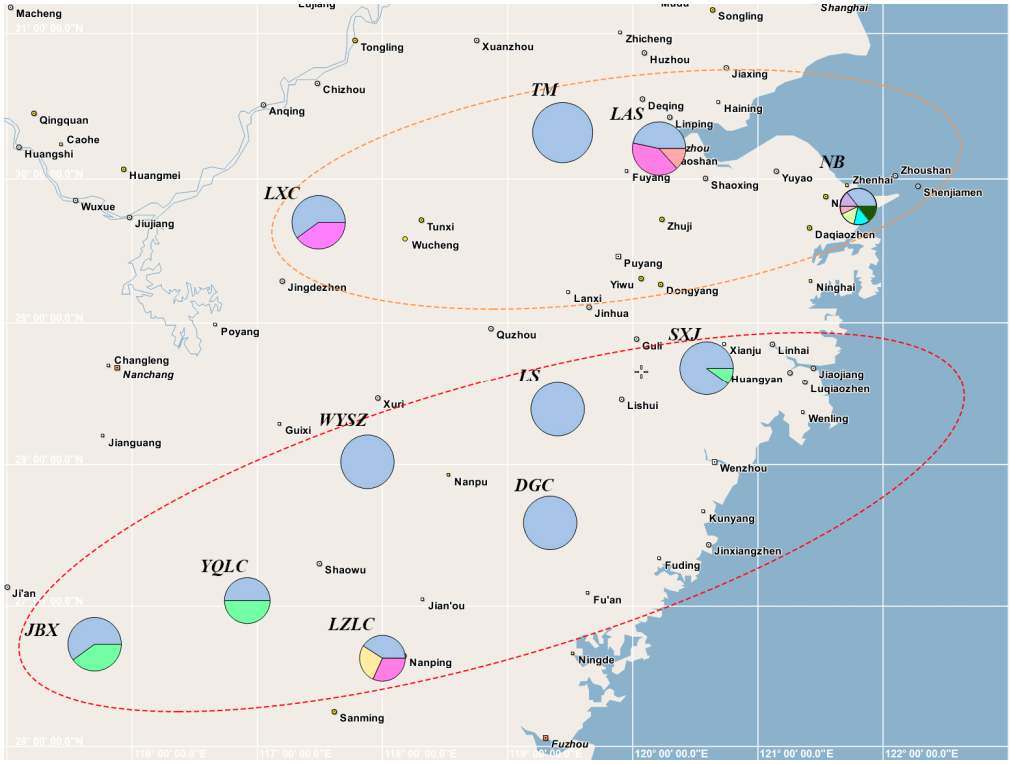

Figure 1. Geographical distribution of haplotypes of *Phoebe chekiangensis* based on 3 spacer regions of cpDNA samples. In the figure, pie size, color, and proportion represent population quantity, haplotype, and haplotype count, respectively.

At the regional level, the four populations in the northern region contained nine haplotypes with a total of 112 individuals (35.9%), of which H1 accounted for 67.0% of the populations in this region, making it the predominant haplotype. Following were H3 and H5, each with 12 individuals. In contrast, the seven populations in the southern region contained only four haplotypes, with a total of 194 individuals (64.1%), of which H1 accounted for 79.9% of the populations.

3.3. Haplotype Network

From Figure 2, it can be inferred that haplotype H1 was an ancient haplotype, while the remaining haplotypes were located in the outer branches, suggesting they were derived types. Derived haplotypes evolved independently in parallel, with little exchange. The 11 haplotypes of *Phoebe chekiangensis* could be divided into two distinct branches: a southern branch and a northern branch, which was generally consistent with the geographical distribution.

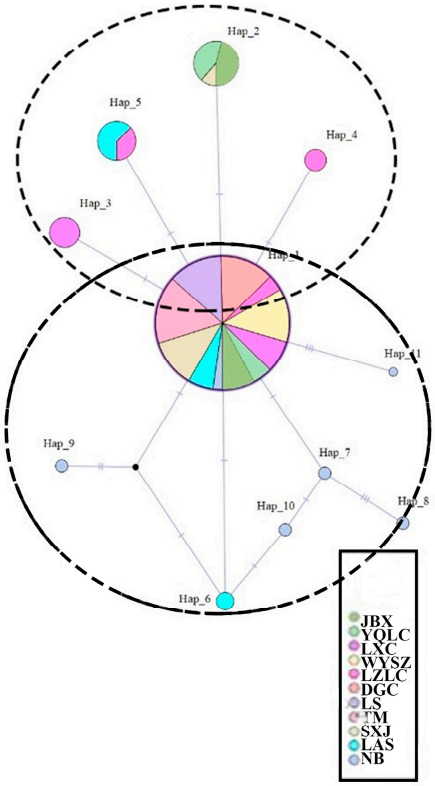

Figure 2. Haplotype TCS network map based on three spacer regions of cpDNA. The legend of the 11 populations uses 11 colors to represent each group, with each circle representing the number of populations contained within a haplotype.

3.4. Spacer Regions of cpDNA Population Genetic Structure

From the perspective of population genetic differentiation, at the species level of *Phoebe chekiangensis*, the population differentiation index based on spacer regions of cpDNA was F_{st} = 0.25610 ($p < 0.05$), with a gene flow N_m = 0.73, indicating a certain degree of differentiation. The genetic variation between populations was 29.14%, while within populations, it was 70.86%, with lower genetic variation between populations than within populations (Table 5).

Table 5. Molecular variance analyses (AMOVA) utilizing cpDNA spacer regions data for *P. chekiangensis* populations.

Source of Variation	d.f.	Sum of Squares	Variance Components	Percentage of Variation	Fixation Indices	N_m	G_{st}/N_{st}
All populations							
Between populations	10	25.329	0.08409	29.14	F_{st} = 0.25610	0.73	0.28379/0.25597
Within populations	295	60.332	0.20451	70.86			($p < 0.05$)
Southern populations							
Between populations	4	13.307	0.11635	34.08	F_{st} = 0.32531	0.52	0.22590/0.32536
Within populations	129	29.036	0.22509	65.92			($p < 0.05$)
Northern populations							
Between populations	5	9.170	0.05813	23.57	F_{st} = 0.18753	1.08	0.28466/0.18725
Within populations	166	31.295	0.18853	76.43			($p < 0.05$)
Southern regions and Northern regions							
Between regions	1	2.852	0.00172	0.59		F_{SC} = 0.28907	
Within regions	9	22.477	0.08316	28.74		F_{ST} = 0.29328	
Within populations	295	60.332	0.20451	70.67		F_{CT} = 0.00593	

F_{CT}: proportion of genetic variation between groups. F_{SC}: proportion of genetic variation between populations within groups. F_{ST}: proportion of genetic variation between populations and groups overall.

3.5. Analysis of Spacer Regions of cpDNA Haplotype Phylogeny and Evolutionary Time

The phylogenetic results show that taking the *Machilus oreophila* and *Machilus nanmu* of the *Machilus* genus as outgroups, all 11 haplotypes of *Phoebe chekiangensis* formed a highly supported monophyletic clade, with two branches differentiating within the group, which was consistent with the clustering situation in the haplotype network diagram (Figure 2).

The maximum likelihood (ML) haplotype tree shows that haplotypes H6 and H9 diverged as the first branch, corresponding to the northern region, while the other haplotypes clustered into another major branch. In further differentiation, haplotypes H7, H8, and H10 evolved separately as parallel branches, also corresponding to the northern region. The remaining haplotypes H1–H5 and H11 formed parallel branches, including a mixture of both the southern and northern regions. The Bayesian haplotype tree results were largely consistent with the maximum likelihood (ML) haplotype tree, where both supported the separate divergence of haplotypes H7, H8, and H10 as parallel branches in the northern region, and the H6 and H9 haplotypes in the southern region, while the other haplotypes formed parallel branches mixing the northern and southern regions (Figures 3 and 4).

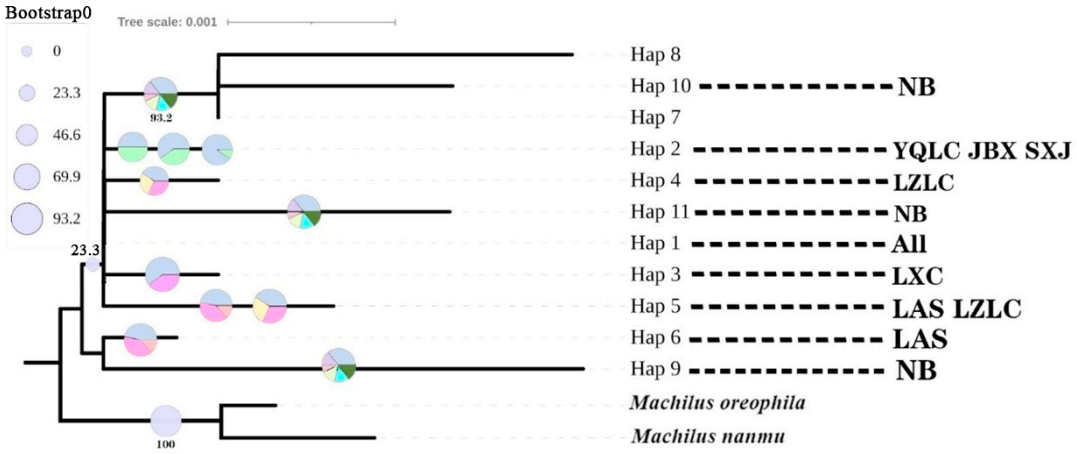

Figure 3. Three cpDNA spacer regions were utilized with maximum likelihood (ML) methods to build haplotype trees (*psbC-trnS*, *trnL-Intro*, *ycf3*).

The divergence time between the *Phoebe* and *Machilus* genera was estimated to be approximately 37.87 mya (PP = 1; 95%HPD: 25.63–44.54 mya), and the crown group time of the *Phoebe* genus was estimated to be 21.30 mya (PP = 1; 95%HPD: 9.76–34.94 mya) (Figure 5).

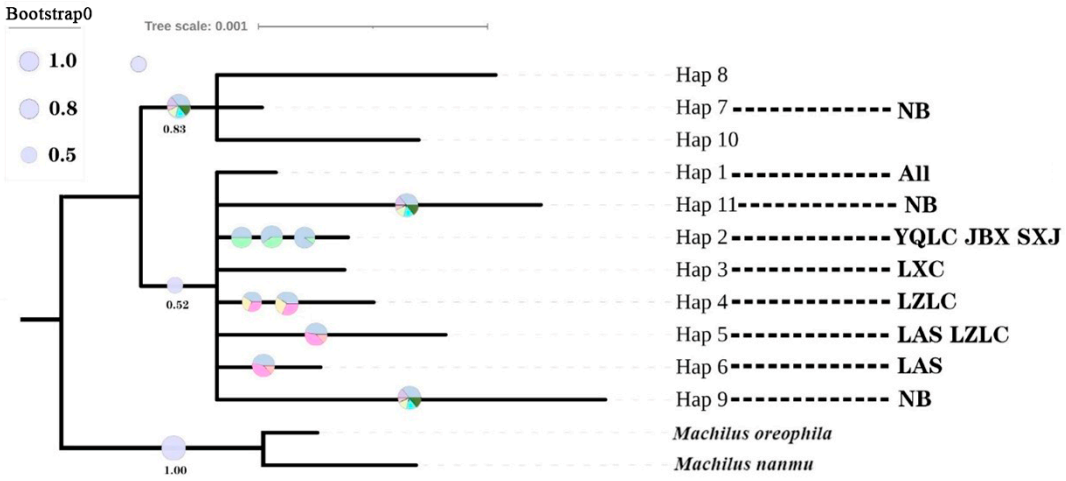

Figure 4. Bayesian inference (BI) haplotype tree was constructed using three cpDNA spacer regions (*psbC-trnS*, *trnL-Intro*, *ycf3*).

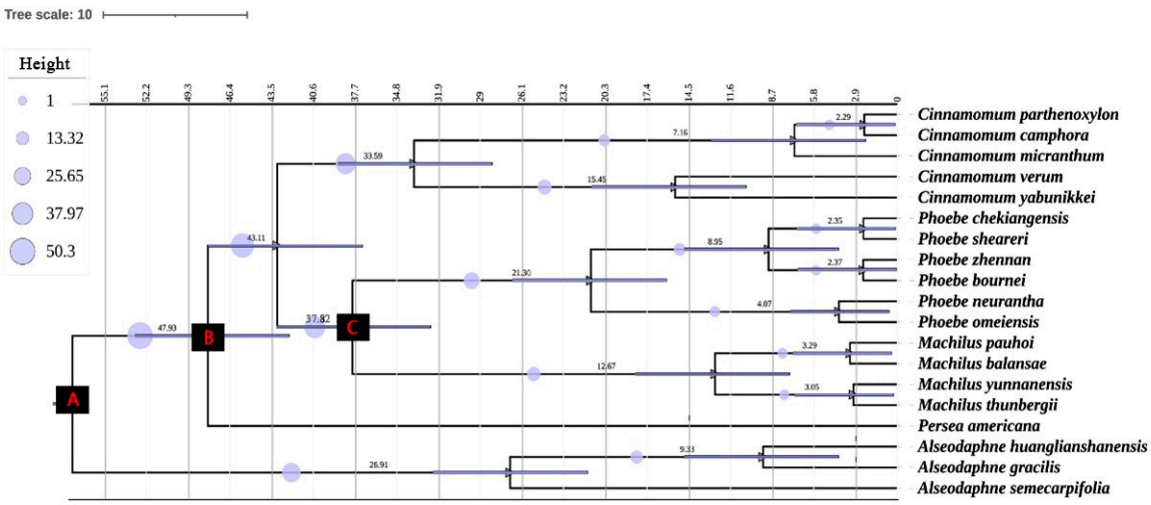

Figure 5. Phylogenetic trees of Lauraceae based on spacer regions of cpDNA (*ycf3*) with 3 time correction points.

The divergence time between the *Machilus* and *Phoebe* (node 3) was used to calibrate the basal part of the intraspecific haplotype time tree, which estimated the common ancestor time of the 11 *Phoebe chekiangensis* haplotypes to be 7.85 mya, which was within the range of the first tree-level time tree [33–35]. The divergence results show that the H7, H8, and H10 haplotypes of *Phoebe chekiangensis* (northern region) differentiated relatively late, with a divergence time of 1.90 mya. The lineage divergence times of the remaining haplotypes were consistent, forming parallel branches (Figure 6, Table 6) [24,36].

Table 6. Summary of cpDNA spacer regions for estimating divergence times using Bayesian methods.

	Node	Fossil References	Minimum Age (mya)	Mean Ages (mya)
A:	Divergence between Laureae and Cinnamomeae	Reid, E.M. et al., 1933 [33]	52	57.33 (41.63, 85.76)
B:	Crown node of the Persea group	Li et al., 2009 [34]; Li, H., 2020 [35]	43	47.93 (42.25, 66.42)
C:	Stem node of Machilus	Li et al., 2016a [36]; Tang et al., 2016 [24]	33.7	37.87 (25.63, 44.54)
1:	*Phoebe chekiangensis*			7.85
2:	H7 + H8 + H10			1.90

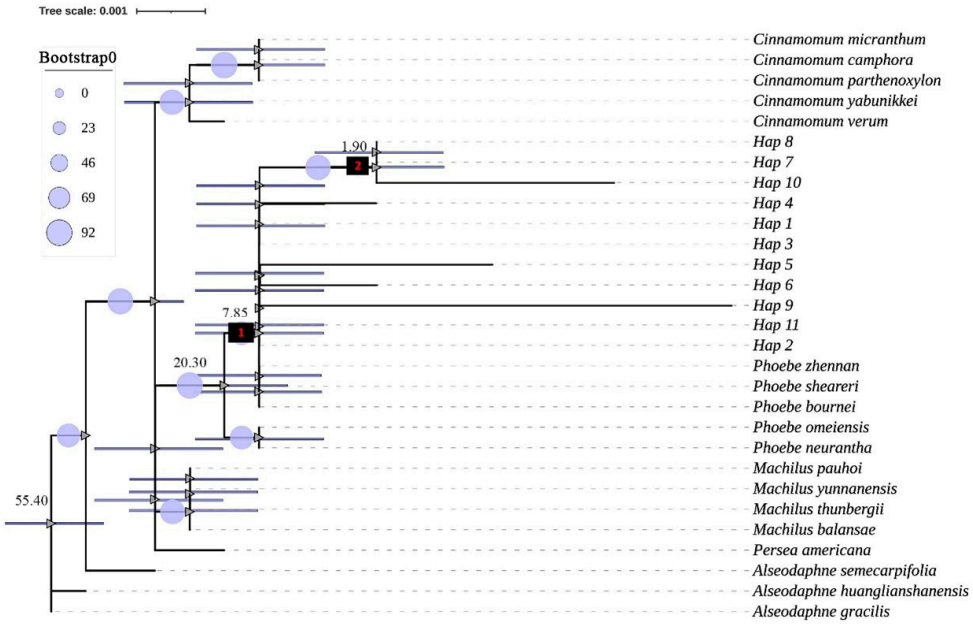

Figure 6. Chronograms of *Phoebe chekiangensis* groups inferred using Bayesian Evolutionary Analysis by Sampling Trees (BEAST) from cpDNA spacer region sequences (*ycf3*).

3.6. Population History Dynamic Analysis

The results show that among the 11 populations of *Phoebe chekiangensis*, only the Tian Tong Shan population in Ningbo (NB) had negative values for Tajima's D and Fu's Fs, but the *p*-value was not statistically significant ($p > 0.05$), suggesting that this population had not experienced recent expansion or a bottleneck event. At the geographic grouping level, both the southern and northern regions had negative values for Tajima's D and Fu's Fs, but only the *p*-value of the northern region was statistically significant ($p < 0.05$) [37]. Thus, it is evident that *Phoebe chekiangensis* had not experienced recent expansion or a bottleneck event at the species level, but at the geographic grouping level, the northern region contradicted the neutral theory, indicating a recent expansion or bottleneck event (Table S1).

The results of the mismatch distribution analysis at the population and geographic levels indicate that the *p*-values for both the sudden and spatial expansion models of the Tian Tong Shan (NB) and Shen Xian Ju (SXJ) populations of *Phoebe chekiangensis*, along with the northern region, were not significant (P(SSD)/P(Rag) > 0.05), indicating acceptance of the spatial expansion model. Furthermore, the mismatch distribution curve (MDC) results (Figure 7) reveal a significant overlap between the observed and expected curves for *Phoebe chekiangensis* at the species level (All) and the northern region population, suggesting a potential historical expansion. Therefore, a population expansion of *Phoebe chekiangensis* occurred (Tables S2–S4).

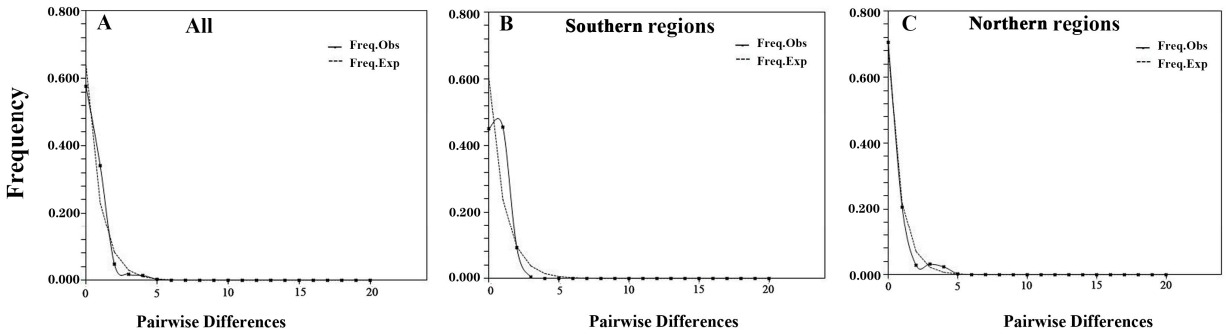

Figure 7. The mismatch distribution map of distinct geographical groups (lineages) of *Phoebe chekiangensis* was generated based on spacer regions of cpDNA fragment analysis.

4. Discussion

4.1. Genetic Diversity and Genetic Differentiation

The genetic variation between populations of woody plants is usually smaller than within populations [14]. Species with large distribution ranges have more genetic diversity, while endemic species have smaller effective population sizes and suffer greater genetic variation loss due to genetic drift during dispersal [38–40]. Therefore, these species exhibit fewer polymorphic loci and lower genetic diversity. Research results show that the spacer regions of cpDNA genetic diversity of the *Phoebe chekiangensis* species, with H_d = 0.423, and nucleotide diversity, with $P_i \times 10^{-3}$ = 0.400, were both lower than the statistical average of 0.670 [14]. This result is consistent with conclusions drawn from ISSR marker studies on *Phoebe chekiangensis*, indicating low genetic diversity in this species [41]. The genetic variation between populations was 29.14%, while within populations, it was 70.86%, with the inter-population genetic variation much lower than the within-population variation, which is consistent with the genetic variation pattern of *Phoebe chekiangensis* based on EST-SSR markers [42]. From a geographic grouping perspective, this indicates a low level of population differentiation between the southern and northern regions of *Phoebe chekiangensis*.

RAPD analysis of the closely related species *Phoebe bournei* shows that genetic variation mainly exists within populations, suggesting that natural selection pressure experienced by *Phoebe bournei* seedlings in their natural state is the main source of individual variation within populations [43]. Actual investigations found similar population structure characteristics in *Phoebe chekiangensis* populations, where genetic diversity analysis results are consistent with population ecological characteristics, suggesting that environmental selection pressure has a similar effect on these two *Phoebe* species. Additionally, frequent human disturbances and fruit dispersal by birds and mammals may also affect the genetic diversity and genetic structure characteristics of *Phoebe chekiangensis* [44].

Overall, the genetic diversity within populations was higher than between populations in the current situation.

4.2. Phylogeographic Structure

Molecular clock estimation indicates that in the late Miocene to early Pliocene, the population gradually differentiated into two lineages due to climate change and geographic isolation, with divergence times consistent with those of *Emmenopterys henryi* (5.06 mya) [40,45,46] and *Machilus thunbergii* (4.39 mya) [47]. The divergence time of representative haplotypes H7, H8, and H10 from the northern lineage was relatively recent (1.90 mya), which occurred in the early Pliocene. During this period, despite significant climate fluctuations, the climate was still relatively warm and humid. It was postulated that after the completion of the final differentiation of these three haplotypes in the population of Ningbo Tiantongshan (NB) during this period, the climate subsequently became drier and colder, hindering their further dispersal to other regions [39]. Represented by H1 and H2, the haplotypes of the southern lineage were ancient and uniform, suggesting a shorter dispersal time and frequent gene flow in the *Phoebe chekiangensis* population in this region, which prevented further differentiation [46]. Overall, the distribution center and basic pattern of the *Phoebe chekiangensis* population were established from the late Miocene to the early Pliocene, extending at the latest to the early Pliocene.

4.3. Historical Dynamics of the Population

The shared ancient haplotype H1 in all populations was exclusively present in Wuyishan Town, Jiangxi (WYSZ); Pankeng Village, Lishui, Zhejiang (LS); and Daigen Village, Zhejiang (DGC), indicating a possible distribution center for *Phoebe chekiangensis*. This area coincides with the local glacial refugia known as "Wuyishan" and "Zhenan" in the East China region, nurturing relict species, like *Abies beshanzuensis*, and serving as a "museum" and "cradle" for woody plants [48]. Simulated distribution during the last glacial maximum suggests this region as the distribution center for *Phoebe chekiangensis*, spreading

primarily northeastward in the mid-Holocene [47]. Throughout the Quaternary period, especially during the alternating cycles of the Pleistocene glaciations and interglacials, the distribution of *Phoebe chekiangensis* may have expanded and contracted on a larger scale, which is a hypothesis that requires further evidence from paleontological and palynological studies [44]. However, the changes in the simulated distribution area during the last glacial maximum and mid-Holocene provide valuable insights into understanding the migration routes of *Phoebe chekiangensis*. It can be inferred that the dispersal pathway of *Phoebe chekiangensis* radiated northeastward from this center, spreading across the Hang-Gan tectonic zone to subtropical regions in the north, reaching Tiantai Mountain, Zhejiang (TM), and Luxicun Village, Anhui (LXC); the dispersal then spread eastward through the Zhejiang Nan mountains to Tiantong Mountain, Ningbo, along the eastern coast of the East China Sea, where multiple haplotypes were formed in new habitats.

The relative richness of the *Phoebe chekiangensis* haplotypes in Tiantong Mountain, Ningbo (NB), was likely due to the significant influence of a maritime climate, which provided a warm and humid environment conducive to the survival and rapid turnover and evolution of *Phoebe chekiangensis*. Within the TWINSPAN classification, the impact of rainfall during the driest season on the community in Tiantong Mountain was the most significant among all the distribution areas. Additionally, confirmation can be sought from the vegetation status in the nearby Zhoushan Islands [49,50]. The Zhoushan Islands, facing the Tiantai Mountain, which includes Tiantong Mountain, across the sea in the Taibai Mountain branch of the Tiantai Mountain range, with a distance of less than 10 km, exhibited high similarity coefficients of plant genera and species at 82.0% and 75.9%, respectively, exceeding those of Tiantai Mountain and the Japanese region at the same latitude. Despite multiple connections and separations from the mainland since the Quaternary glaciation, unique species of Lauraceae like *Neolitsea sericea* and *Cinnamomum japonicum* var. *chenii* have evolved in the Zhoushan Islands [51]. This has been likely due to the influence of a maritime climate, resulting in distinctive regional characteristics of the East Asian plant flora and a strong tropical affinity, leading to the rapid evolution of Lauraceae plants with high species turnover rates, generating new species within a short period [52].

5. Conclusions

As a hotspot of global biodiversity, the subtropical region serves as an important refuge for evolutionary lineages from the Middle Miocene to the Late Miocene and is also an area with extremely high plant richness and endemism [49]. The current genetic structure of species and populations has mainly been shaped by the Quaternary Ice Age, and the geographic distribution and genetic structure of *Phoebe chekiangensis* have also been shaped under such an influence [53]. Based on the current distribution records of *Phoebe chekiangensis*, it was observed that *Phoebe chekiangensis* was less adapted to the central subtropical region compared with the northern subtropical regions, which is a proposition supported by simulated distributions during the last glacial maximum and mid-Holocene [44,54–56]. Therefore, despite the primary dispersal of *Phoebe chekiangensis* southward along Wuyishan, forming new haplotypes in their respective habitats, the consistency and uniformity of haplotypes in Yanquanlinchang, Fuzhou, Jiangxi (YQLC), and Junbu Township, Yongfeng, Jiangxi (JBX), as well as the results of neutrality tests (NTs) and mismatch distribution analysis (MDA), suggest that the time frame for *Phoebe chekiangensis* to expand southwestward along Wuyishan was relatively short and its adaptability to the environment was low, thereby limiting the formation of new haplotypes. The cultivated population in Shenxianju, Taizhou (SXJ), may have originated from the populations in Yanquanlinchang (YQLC) or Junbu Township (JBX) [57].

Supplementary Materials: The following supporting information can be downloaded from https://www.mdpi.com/article/10.3390/f15071073/s1: Table S1. Neutrality test for populations of *Phoebe chekiangensis*; Table S2. Neutrality test for four geographical groups of *Phoebe chekiangensis*; Table S3. Mismatch distribution analysis (MDA) of *Phoebe chekiangensis*; Table S4. Mismatch distribution analysis (MDA) of *Phoebe chekiangensis*.

Author Contributions: Conceptualization: X.W. Sample collection: X.W., Y.C. and C.N. Data curation: X.W., Y.C., C.N., S.G. and X.C. Valuable advice: X.Y. Writing—review and editing: X.W. All authors have read and agreed to the published version of the manuscript.

Funding: This study was funded by Science and Technology Project of the Nanjing Greening and Landscaping Bureau (project number: YLK202211JH): Investigation of *Phoebe hunanensis* germplasm resources and research on seedling cultivation techniques.

Data Availability Statement: Data is contained within the article.

Acknowledgments: We thank Xiangui Yi, Yan Chen, and Chenhui Nan for their help in the field, and Lin Chen and Jing Qiu for their valuable suggestions regarding the data analysis.

Conflicts of Interest: The authors declare no conflicts of interest.

References

1. Li, S.; Li, X.W.; Li, J.; Huang, P.H.; Wei, F.N.; Cui, H.B.; van der Werff, H. Lauraceae. In *Flora of China*; Wu, Z.Y., Raven, P.H., Hong, D.Y., Eds.; Science Press: Beijing, China; Missorui Botanical Garden Press: St. Louis, MO, USA, 2008; Volume 7, pp. 102–254.
2. Gao, J.H.; Zhang, W.; Li, J.Y.; Long, H.L.; He, W.; Li, X.Q. Amplified fragment length polymorphism analysis of the population structure and genetic diversity of *Phoebe zhennan* (Lauraceae), a native species to China. *Biochem. Syst. Ecol.* **2016**, *64*, 149–155. [CrossRef]
3. Li, Y.G.; Liu, X.H.; Ma, J.W.; Shi, C.G.; Zhu, G.Q. Phenotypic variations in populations of *Phoebe chekiangensis*. *Chin. J. Plant Ecol.* **2014**, *38*, 1315–1324. [CrossRef]
4. Hong, C.; Shi, W.; Wu, S.; He, Y.; Ying, Y. The inferior root plasticity of *Phoebe chekiangensis* and *Torreya grandis* seedlings intercropped with Phyllostachys edulis leads to worse plant performance than monocultures under shade conditions. *Plant Soil* **2023**, *488*, 305–324. [CrossRef]
5. Jump, A.S.; Marchant, R.; Peñuelas, J. Environmental change and the option value of genetic diversity. *Trends Plant. Sci.* **2009**, *14*, 51–58. [CrossRef]
6. Hoban, S.; Bruford, M.; D'Urban Jackson, J.; Lopes-Fernandes, M.; Heuertz, M.; Hohenlohe, P.A.; Paz-Vinas, I.; Sjögren-Gulve, P.; Segelbacher, G.; Vernesi, C.; et al. Genetic diversity targets and indicators in the CBD post-2020 Global Biodiversity Framework must be improved. *Biol. Conserv.* **2020**, *248*, 108654. [CrossRef]
7. Birky, C.W. Uniparental Inheritance of Mitochondrial and Chloroplast Genes-Mechanisms and Evolution. *Proc. Natl. Acad. Sci. USA* **1995**, *92*, 11331–11338. [CrossRef]
8. Jansen, R.K.; Cai, Z.; Raubeson, L.A.; Daniell, H.; Depamphilis, C.W.; Leebens-Mack, J.; Müller, K.F.; Guisinger-Bellian, M.; Haberle, R.C.; Hansen, A.K.; et al. Analysis of 81 Genes from 64 Plastid Genomes Resolves Relationships in Angiosperms and Identifes Genome-Scale Evolutionary Patterns. *Proc. Natl. Acad. Sci. USA* **2007**, *104*, 19369–19374. [CrossRef]
9. Avise, J.C.; Arnold, J.; Ball, R.M.; Bermingham, E.; Lamb, T.; Neigel, J.E.; Reeb, C.A.; Saunders, N.C. Intraspecific phylogeography: The mitochondrial DNA bridge between population genetics and systematics. *Annu. Rev. Ecol. Syst.* **1987**, *18*, 489–522. [CrossRef]
10. Li, S.; Liu, S.; Pei, S.; Ning, M.; Tang, S. Genetic diversity and population structure of *Camellia huana* (Theaceae), a limestone species with narrow geographic range, based on chloroplast DNA sequence and microsatellite markers. *Plant. Divers.* **2020**, *42*, 343–350. [CrossRef]
11. Kavaliauskas, D.; Danusevičius, D.; Baliuckas, V. New Insight into Genetic Structure and Diversity of Scots Pine (*Pinus sylvestris* L.) Populations in Lithuania Based on Nuclear, Chloroplast and Mitochondrial DNA Markers. *Forests* **2022**, *13*, 1179. [CrossRef]
12. Dong, J.; Yi, X.; Wang, X.; Li, M.; Chen, X.; Gao, S.; Fu, W.; Qian, S.; Zeng, X.; Yun, Y. Population Variation and Phylogeography of Cherry Blossom (*Prunus conradinae*) in China. *Plants* **2024**, *13*, 974. [CrossRef]
13. Phumichai, C.; Phumichai, T.; Wongkaew, A. Novel Chloroplast Microsatellite (cpSSR) Markers for Genetic Diversity Assessment of Cultivated and Wild Hevea Rubber. *Plant Mol. Biol. Rep.* **2015**, *33*, 1486–1498. [CrossRef]
14. Petit, R.J.; Duminil, J.; Fineschi, S.; Hampe, A.; Salvini, D.; Vendramin, G.G. INVITED REVIEW: Comparative organization of chloroplast, mitochondrial and nuclear diversity in plant populations. *Mol. Ecol.* **2005**, *14*, 689–701. [CrossRef]
15. Ribeiro, R.A.; Lemos-Filho, J.P.; Ramos, A.C.S.; Lovato, M.B. Phylogeography of the endangered rosewood *Dalbergia nigra* (Fabaceae): Insights into the evolutionary history and conservation of the Brazilian Atlantic Forest. *Heredity* **2011**, *106*, 46–57. [CrossRef]
16. Young, A.; Boyle, T.; Brow, T. The population genetic consequences of habitat fragmentation for plants. *Trends Ecol. Evol.* **1996**, *11*, 413–418. [CrossRef]
17. Pironon, S.; Villellas, J.; Morris, W.F.; Doak, D.F.; García, M.B. Do geographic, climatic or historical ranges differentiate the performance of central versus peripheral populations? *Glob. Ecol. Biogeogr.* **2015**, *24*, 611–620. [CrossRef]
18. Makhmudjanov, D.; Abdullaev, D.; Juramurodov, I.; Tuychiev, S.; Yusupov, Z.; Sun, H.; Tojibaev, K.; Deng, T. Comparative Analysis and Characterization of Ten Complete Chloroplast Genomes of *Eremurus* Species (Asphodelaceae). *Forests* **2023**, *14*, 1709. [CrossRef]
19. Gapare, W.J.; Aitken, S.N. Strong spatial genetic structure in peripheral but not core populations of Sitka spruce [*Picea sitchensis* (Bong.) Carr.]. *Mol. Ecol.* **2005**, *14*, 2659–2667. [CrossRef]

20. Alawfi, M.S.; Albokhari, E.J. Comparative Chloroplast Genomics Reveals a Unique Gene Inversion in Two *Cordia* Trees (Cordiaceae). *Forests* **2023**, *14*, 1778. [CrossRef]
21. Zhu, H.; Liu, J.; Li, H.; Yue, C.; Gao, M. Complete Chloroplast Genome Structural Characterization and Comparative Analysis of *Viburnum japonicum* (Adoxaceae). *Forests* **2023**, *14*, 1819. [CrossRef]
22. Castro, J.C.; Rodríguez, H.N.; Maddox, J.D.; Jiu, B.; Petterman, J.B.; Marapara, J.L.; Cobos, M. A simple and efficient method for high-quality total RNA isolation from Oleaginous microalgae. *Plant Cell Biotechnol. Mol. Biol.* **2017**, *18*, 15–21.
23. Qiao, M.; Chen, B.; Fu, Y. Identification of Five Wood Species of *Phoebe* and *Machilus* based on DNA. *Genom. Appl. Biol.* **2018**, *37*, 4013–4021.
24. Tang, B.; Han, M.; Xu, Q.Q.; Jin, J.H. Leaf cuticle microstructure of *Machilus maomingensis* sp. nov. (Lauraceae) from the Eocene of the Maoming Basin, South China. *Acta Geol. Sin.* **2016**, *90*, 1561–1571. [CrossRef]
25. Katoh, K.; Standley, D.M. MAFFT multiple sequence alignment software version 7: Improvements in performance and usability. *Mol. Biol. Evol.* **2013**, *30*, 772–780. [CrossRef] [PubMed]
26. Bandelt, H.J.; Forster, P.; Rohl, A. Median-joining networks for inferring intraspecific phylogenies. *Mol. Biol. Evol.* **1999**, *16*, 37–48. [CrossRef] [PubMed]
27. Excoffier, L.; Lischer, H.E. Arlequin suite version 3.5: A new series of programs to perform population genetics analyses under Linux and Windows. *Mol. Ecol. Resour.* **2010**, *10*, 564–567. [CrossRef] [PubMed]
28. Swofford, D.L. *PAUP: Phylogenetic Analysis Using Parsimony (and Other Methods) 4.0 Beta*; Sinauer Associates: Sunderland, MA, USA, 2002.
29. Ronquist, F.; Huelsenbeck, J.P. MrBayes 3: Bayesian phylogenetic inference under mixed models. *Bioinformatics* **2003**, *19*, 1572–1574. [CrossRef] [PubMed]
30. Rambaut, A. *FigTree v1. 4.0. A Graphical Viewer of Phylogenetic Trees*; Institute of Evolutionary Biology, University of Edinburgh: Edinburgh, UK, 2012.
31. Drummond, A.J.; Suchard, M.A.; Xie, D.; Rambaut, A. Bayesian phylogenetics with BEAUti and the BEAST 1.7. *Mol. Biol. Evol.* **2012**, *29*, 1969–1973. [CrossRef] [PubMed]
32. Rambaut, A.; Suchard, M.A.; Xie, D.; Drummond, A.J. Tracer v1.6. 2014. Available online: http://beast.bio.ed.ac.uk/Tracer (accessed on 31 January 2017).
33. Reid, E.M.; Chandler, M.E.J. *The London Clay Flora*; British Museum (Natural History): London, UK, 1933; p. 200.
34. Li, J.Z.; Qiu, J.; Liao, W.B.; Jin, J.H. Eocene fossil Alseodaphne from Hainan Island of China and its paleoclimatic implications. *Sci. China Ser. D Earth Sci.* **2009**, *52*, 1537–1542. [CrossRef]
35. Li, H.; Liu, B.; Davis, C.C.; Yang, Y. Plastome phylogenomics, systematics, and divergence time estimation of the *Beilschmiedia* group (Lauraceae). *Mol. Phylogenetics Evol.* **2020**, *151*, 106901. [CrossRef] [PubMed]
36. Li, L.; Madriñán, S.; Li, J. Phylogeny and biogeography of *Caryodaphnopsis* (Lauraceae) inferred from low-copy nuclear gene and ITS equences. *Taxon* **2016**, *65*, 433–443. [CrossRef]
37. Pilkington, M.M.; Wilder, J.A.; Mendez, F.L.; Cox, M.P.; Woerner, A.; Angui, T.; Kingan, S.; Mobasher, Z.; Batini, C.; Destro-Bisol, G.; et al. Contrasting signatures of population growth for mitochondrial DNA and Y chromosomes among human populations in Africa. *Mol. Biol. Evol.* **2008**, *25*, 517–525. [CrossRef] [PubMed]
38. Hamrick, J.L.; Godt, M.J.W. Effects of Life History Traits on Genetic Diversity in Plant Species. *Philos. Trans. Biol. Sci.* **1996**, *351*, 1291–1298.
39. Varvio, S.L.; Chakraborty, R.; Nei, M. Genetic variation in subdivided populations and conservation genetics. *Heredity* **1986**, *57*, 189–198. [CrossRef] [PubMed]
40. Qiu, Y.X.; Guan, B.C.; Fu, C.X.; Comes, H.P. Did glacials and/or interglacials promote allopatric incipient speciation in East Asian temperate plants? Phylogeographic and coalescent analyses on refugial isolation and divergence in Dysosma versipellis. *Mol. Phylogenetics Evol.* **2009**, *51*, 281–293. [CrossRef] [PubMed]
41. Zhang, R.; Zhou, Z.; Jin, G.; Wang, S.; Wang, X. Genetic diversity and differentiation within three species of the family Lauraceae in southeast China. *Biochem. Syst. Ecol.* **2012**, *44*, 317–324. [CrossRef]
42. Ding, Y.; Zhang, J.; Lu, Y.F.; Lin, E.; Lou, L.; Tong, Z. Development of EST-SSR markers and analysis of genetic diversity in natural populations of endemic and endangered plant *Phoebe chekiangensis*. *Biochem. Syst. Ecology.* **2015**, *63*, 183–189. [CrossRef]
43. Jiang, X.; Wen, Q.; Ye, J.; Xiao, F.; Jiang, M. RAPD analysis on genetic diversity in eight natural populations of *Phoebe bournei* from Fujian and Jiangxi Province, China. *Acta Ecol. Sin.* **2009**, *29*, 438–444.
44. Chen, S.P.; Sun, W.H.; Xiong, Y.F.; Jiang, Y.T.; Liu, X.D.; Liao, X.Y.; Zhang, D.Y.; Jiang, S.Z.; Li, Y.; Liu, B.; et al. The *Phoebe* genome sheds light on the evolution of magnoliids. *Hortic. Res.* **2020**, *7*, 146. [CrossRef] [PubMed]
45. Chen, L.; Pan, T.; Qian, H.; Zhang, M.; Yang, G.; Wang, X. Genetic Diversity and Population Structure Revealed by SSR Markers on Endemic Species *Osmanthusserrulatus* Rehder from Southwestern Sichuan Basin, China. *Forests* **2021**, *12*, 1365. [CrossRef]
46. Wang, Y.H.; Jiang, W.M.; Comes, H.P.; Hu, F.S.; Qiu, Y.X.; Fu, C.X. Molecular phylogeography and ecological niche modelling of a widespread herbaceous climber, *Tetrastigma hemsleyanum* (Vitaceae): Insights into Plio-Pleistocene range dynamics of evergreen forest in subtropical China. *New Phytol.* **2015**, *206*, 852–867. [CrossRef] [PubMed]
47. Leng, X.; Wang, Z.S.; An, S.Q.; Wang, G.M.; Zheng, J.W.; Feng, J. The Influence of Insular Geographical Isolation on Population Genetic Structure of *Machilus thunbergii*. *J. Nanjing For. Univ.* **2006**, *30*, 20–24.

48. Stuart, Y.E.; Losos, J.B.; Algar, A.C. The island–mainland species turnover relationship. *Proc. R. Soc. B Biol. Sci.* **2012**, *279*, 4071–4077. [CrossRef] [PubMed]
49. Wan, L.Q.; Ding, B.Y.; Guo, S.L. Difference of spermatophyte flora among main islands of Zhoushan archipelago and its influencing factors. *J. Zhejiang Univ.* **2008**, *34*, 677–683. [CrossRef]
50. Lu, L.M.; Mao, L.F.; Yang, T.; Ye, J.F.; Liu, B.; Li, H.L.; Sun, M.; Miller, J.T.; Mathews, S.; Hu, H.H.; et al. Evolutionary history of the angiosperm flora of China. *Nature* **2018**, *554*, 234–238. [CrossRef] [PubMed]
51. Zhang, Q.; Chiang, T.; George, M.; Liu, J.Q.; Abbott, R.J. Phylogeography of the Qinghai-Tibetan Plateau endemic *Juniperus przewalskii* (Cupressaceae) inferred from chloroplast DNA sequence variation. *Mol. Ecol.* **2010**, *14*, 3513–3524. [CrossRef] [PubMed]
52. Mona, S.; Ray, N.; Arenas, M.; Excoffier, L. Genetic consequences of habitat fragmentation during a range expansion. *Heredity* **2014**, *112*, 291–299. [CrossRef] [PubMed]
53. Xu, J.; Deng, M.; Jiang, X.L.; Westwood, M.; Song, Y.G.; Turkington, R. Phylogeography of *Quercus glauca* (Fagaceae), a dominant tree of East Asian subtropical evergreen forests, based on three chloroplast DNA interspace sequences. *Tree Genet. Genomes* **2015**, *11*, 805. [CrossRef]
54. Royden, L.H.; Burchfiel, B.C.; Van Der Hilst, R.D. The geological evolution of the Tibetan Plateau. *Science* **2008**, *321*, 1054–1058. [CrossRef] [PubMed]
55. Zhang, H.J.; Feng, T.; Landis, J.B.; Deng, T.; Zhang, X.; Meng, A.P.; Sun, H.; Wang, H.C.; Sun, Y.X. Molecular phylogeography and ecological niche modeling of *Sibbaldia procumbens* s.l. (Rosaceae). *Front. Genet.* **2019**, *10*, 201. [CrossRef] [PubMed]
56. Gao, Y.D.; Zhang, Y.; Gao, X.F.; Zhu, Z.M. Pleistocene glaciations, demographic expansion and subsequent isolation promoted morphological heterogeneity: A phylogeographic study of the alpine *Rosa sericea* complex (Rosaceae). *Sci. Rep.* **2015**, *5*, 11698. [CrossRef] [PubMed]
57. He, H.; Gao, H.; Xue, X.; Ren, J.; Chen, X.; Niu, B. Variation of sugar compounds in *Phoebe chekiangensis* seeds during natural desiccation. *PLoS ONE* **2024**, *19*, e0299669. [CrossRef] [PubMed]